Journal Pre-proofs

Electron paramagnetic resonance of sonicated powder suspensions in organic solvents

Héla Laajimi, Michela Mattia, Robin S. Stein, Claudia L. Bianchi, Daria C. Boffito

PII: S1350-4177(21)00086-9
DOI: https://doi.org/10.1016/j.ultsonch.2021.105544
Reference: ULTSON 105544

To appear in: *Ultrasonics Sonochemistry*

Received Date: 8 February 2021
Revised Date: 20 March 2021
Accepted Date: 23 March 2021

Please cite this article as: H. Laajimi, M. Mattia, R.S. Stein, C.L. Bianchi, D.C. Boffito, Electron paramagnetic resonance of sonicated powder suspensions in organic solvents, *Ultrasonics Sonochemistry* (2021), doi: https://doi.org/10.1016/j.ultsonch.2021.105544

Electron paramagnetic resonance of sonicated powder suspensions in organic solvents

*Héla Laajimi[a], Michela Mattia[b], Robin S. Stein[c], Claudia L. Bianchi[b], Daria C. Boffito[a,]**

[a]Polytechnique Montréal – Department of Chemical Engineering, C.P. 6079, Centre ville H3C 3A7 Montréal (QC) Canada

[b]Università degli Studi di Milano – Chemistry Department, via Golgi 19, 20133, Milan, Italy

[c]McGill University– Chemistry Department, 801 Rue Sherbrooke Ouest, Montréal, QC H3A 0B8 (QC) Canada

*corresponding author: daria-camilla.boffito@polymtl.ca, tel: (514) 340-4711 ext. 2446.

Highlights

- We sonicated trimethylene and propylene glycol in presence of silica particles
- EPR spectroscopy identified and quantified the generated radicals
- Radical concentration with 12-26 μm is twice as much as with 0.005-0.015 μm SiO_2
- 0.5% wt. 12-26 μm particles, generates more radicals than 3% wt. particles

Abstract

The chemical effects of the acoustic cavitation generated by ultrasound translates into the production of highly reactive radicals. Acoustic cavitation is widely explored in aqueous solutions but it remains poorly studied in organic liquids and in particular in liquid/solid media. However, several heterogeneous catalysis reactions take place in organic solvents.

Thus, we sonicated trimethylene glycol and propylene glycol in the presence of silica particles (SiO_2) of different sizes (5-15 nm, 0.2-0.3 μm, 12-26 μm) and amounts (0.5 wt% and 3 wt%) at an ultrasound frequency of 20 kHz to quantify the radicals generated. The spin trap 5,5-dimethyl-1-pyrrolin–N-oxide (DMPO) was used to trap the generated radicals for study by electron paramagnetic resonance (EPR) spectroscopy. We identified the trapped radical as the hydroxyalkyl radical adduct of DMPO, and we quantified it using stable radical 2,2,6,6-tetramethyl-1-piperidinyloxy (TEMPO) as a quantitation standard. The concentration of DMPO spin adducts in solutions containing silica size 12-26 μm was higher than the solution without particles. The presence of these particles increased the concentration of the acoustically generated radicals by a factor of 1.5 (29 μM for 0.5 wt% of SiO_2 size 12-26 μm vs 19 μM for 0 wt%, after 60 min of sonication). Ultrasound produced fewest radicals in solutions with the smallest particles; the concentration of radical adducts was highest for SiO_2 particle size 12-26 μm at 0.5 wt% loading, reaching 29 μM after 60 min sonication. Ultrasound power of 50.6 W produced more radicals than 24.7 W (23 μM and 18 μM, respectively, at 30 min sonication). Increased temperature during sonication generated more radical adducts in the medium (26 μM at 75 °C and 18 μM at 61 °C after 30 min sonication). Acoustic cavitation, in the presence of silica, increased the production of radical species in the studied organic medium.

Keywords: EPR, spin trapping; ultrasound; free radicals; solid particle; organic solvent; sonochemical activity quantification

1. Introduction

Low-frequency ultrasound (US, 20 kHz to 120 kHz) finds applications as a process intensification technology in many fields such as chemical synthesis (in homogenous and heterogeneous systems) [1,2], food industry [3,4], pharmaceutical [5,6], water treatment [7,8,9], biotechnology [10], polymer chemistry [11]. When combined with heterogeneous catalysis, US promotes and accelerates reactions, and increases the yield of organic syntheses through cavitation [12].

Acoustic cavitation is the formation, growth, and implosive collapse of bubbles in a liquid irradiated with ultrasound [13]. When sound waves pass through the liquid, they generate areas of compression (positive pressure) and expansion (negative pressure). At very low pressure in the expanding region, the intermolecular spaces exceed the critical molecular distance and voids or microbubbles form in the liquid [14]. The size of these vapor-filled cavities oscillates in phase with the compression and expansion cycles (stable cavitation), growing under the effect of the sound pressure field [15]. Over a few cycles, they grow and reach an unstable size and implode violently, releasing phenomenal energy over a very short period of time (100 ns): the pressure and the temperature reach locally about 1000 MPa and 3000 °C, respectively [16–18]. At these conditions, the molecules trapped in the cavitating bubbles dissociate and generate radical plasma. In addition, cavitation induces local turbulence and microcirculation of the liquid thereby improving heat transfer locally and mass transfer both microscopically and macroscopically [19]. The combination of the chemical and mechanical effects of cavitation initiates and propagates chemical reactions [20]. Furthermore, ultrasonic cavitation creates small droplets of two immiscible or partially immiscible phases, which significantly increases the surface available for the reaction between two phases and accelerates the reaction rate [21].

Various sonochemical dosimetry methods measure the acoustic activity by detecting hydroxyl radicals; such as the terephthalate dosimeter (which reacts with hydroxyl radicals to generate 2-hydroxyterephthalate) [19, 22], the Fricke dosimeter (whereby hydroxyl radicals oxidize Fe^{2+} in acid solution) [23–25] and the Weissler dosimeter (where molecular iodine forms from a series of reactions involving iodide and hydroxyl radicals) [15, 26, 27]. Rajamma et al. [28] recently reviewed the Weissler [29], Fricke [30] and terephthalic acid [31] methods. Under the same conditions, they observed that the first two methods detect a higher •OH radical yield than the terephthalic acid method. This was partially, but not fully, explained by the presence of additional hydroxylated products in the case of the first two methods. The reliability of the Weissler and Fricke dosimeters is therefore called into question because of the involvement of the hydroxylated

product that can lead to an overestimation of the concentration of •OH radical generated during sonication. The authors conclude that, however, these dosimetry methods remain key to quantify the relative difference in acoustic activity of a system working at different operating conditions. The application of these dosimeters is limited to water and only quantifies hydroxyl radicals.

There are other methods for quantifying other radicals, such as sonoluminescence [32], subharmonic analysis [33], laser holography [34], and electron spin resonance (ESR) or electron paramagnetic resonance (EPR) [35]. EPR spectroscopy utilizes microwave absorption of paramagnetic species in a magnetic field to characterize and quantify them. Free radicals are often key intermediates in chemical reactions, but their high reactivity means shorter lifetimes and low average concentration detectable by EPR [36]. The spin trapping method is a technique employed to stabilize the short-lived radicals; the radical reacts with the spin trap forming a more stable covalent paramagnetic adduct (spin adduct), which is EPR observable. The EPR spectra of the spin adducts allow the quantification and the identification of the spin trapped radicals [37].

In addition, the spin-trapping technique increases the chance of detecting radicals due to the integrative nature of the spin-trapping process: the rate of spin adduct formation is much higher than the rate of spin adduct decay, and therefore there is a gradual build-up of trapped radicals [38]. Various cyclic nitrones such as 5,5-dimethyl-1-pyrrolin–N-oxide (DMPO) have been successfully exploited in spin trapping experiments [38]–[40]. DMPO is effective in trapping alkyl *(*R•*)*, hydroxyl (•OH) and alkoxy (•OR*)* radicals (Figure 1)*,* because the presence of the two β-methyl groups hinders the disproportionation of the resulting spin adducts, thus rendering them more stable [41], [42].

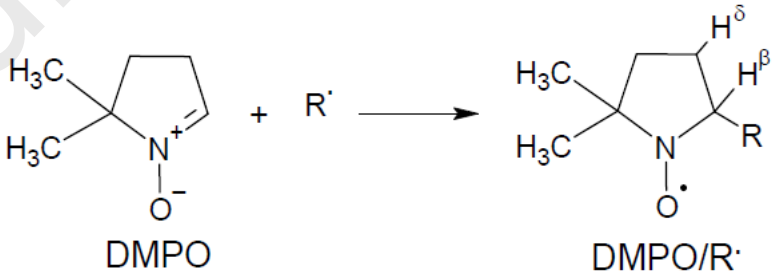

Figure 1: DMPO spin trapping

In the literature, most sonolysis studies by EPR have been conducted in water. Xu et al. [43] identified reactive radicals ($SO_4^{\bullet-}$ and $^{\bullet}OH$) with EPR using DMPO spin trapping to analyze the mechanisms of interactions between ultrasound and peroxymonosulfate on the degradation of pollutants in water. Wei and coworkers [44] applied EPR to examine the kinetics and mechanism of ultrasonic activation of persulfate. They measured the hydroxyl radical ($^{\bullet}OH$) and sulfate radical anion ($SO_4^{\bullet-}$) yield using DMPO as a spin trap. Migik and Riesz [38] identified radical intermediates formed during the sonolysis of some organic liquids and aqueous solutions. In organic liquids, they adopted nitrosodurene and 2,4,6-tri-tert-butylnitrosobenzene as nitroso spin traps. Castellanos et al. [45] investigated the sonolysis of water and ethylene glycol, methanol, and chloroform by EPR-spin trapping at 20 kHz and 475 kHz. The nature of the detected radicals spin adducts was dependent on the sonication time or ultrasound frequency.

Despite ultrasound as a process intensification technique being increasingly applied to mixtures containing solids, especially catalysts, there is a lack of literature on the quantification of chemical effects of ultrasound in the presence of powders. Quantifying these effects would aid in identifying synergies in process intensification and catalysis, maximizing yields and selectivity, and decreasing energy requirements [46].

Barchouchi et al. [47] recently investigated the effect of the presence of solids (glass beads) on acoustic activity at frequency from 20 kHz to 1135 kHz. The glass beads were used in concentrations ranging from 3.2×10^{-3} to 80 $g\cdot L^{-1}$ and with sizes between 8-12 and 6000 µm in diameter. While the calorimetric quantification (measurement of the power rate dissipated in the solution) did not seem affected by the particles, the chemical activity (Weissler method) sharply decreased beyond a certain surface area value. Barchouchi et al. [47] also reviewed previous work done on the determination of the acoustic activity in heterogeneous media. All these data were gathered in water and still, the literature on the subject remains limited.

In this work, we assessed for the first time the chemical effects of acoustic cavitation by identifying and quantifying the free radicals generated when bubbles implode in organic slurry solutions. In this research, EPR quantified the acoustically generated radicals, trapped by DMPO, in organic solvents (propylene glycol and trimethylene glycol) and in the presence of solids (SiO_2) of different particles size (5-15 nm, 0.2-0.3 µm, 12-26 µm). We chose these two organic solvents because in subsequent work we will transesterify vegetable oils with propylene-glycols to produce di-ester

biolubricants. Our goal is to relate the acoustic yield to the conversion and selectivity towards biolubricants to minimize energy requirements.

We chose EPR because of its high sensitivity, specificity, and the simplicity of sample preparation. Moreover, it requires small aliquots of sample [48]. For instance, Abbas et al. [49] could detect a concentration of radicals between 2 and 3 μM for a 25 μL sample, using conventional X-band with a frequency of about 9.4 GHz [50]. Besides investigating the acoustic activity in the two different solvents in the presence of SiO_2, we also quantified the effects of the ultrasonic power and the temperature, in order to identify the optimal conditions to intensify the heterogeneous reaction associated with ultrasound.

2. Materials and methods

2.1. Sonolysis experiments

A 500 W nominal power ultrasonic processor (Sonics & Materials, Inc., Newtown, USA) and a solid probe (1.3 cm tip diameter, 25.4 cm length) sonicated a 50 mL of trimethylene glycol or propylene glycol (Sigma-Aldrich , St. Louis, Mo, USA). The glycol solution was at a concentration of 8 mM of the spin trap 5,5-Dimethyl-1-pyrroline N-oxide (≥97.0% DMPO, Fisher Scientific, Waltham, MA, USA). The processor operated at a fixed frequency of 20 kHz. The sonolysis experiments occurred in a 100 mL jacketed glass reactor (inner diameter = 4 cm, height = 10 cm) in the presence of SiO_2 particles (Sigma-Aldrich) of various sizes (5-15 nm, 0.2-0.3 μm, 12-26 μm) and concentration (0.5 wt% and 3 wt%). A Fisher Brand™ (Ottawa, Ontario) thermostatic bath with water circulation connected to the jacket of the reactor maintained the temperature constant (62 ± 1 °C or 74 ± 1 °C). The irradiation time was 60 min with continuous ultrasonic irradiation. We sampled 40 μL of solution every 10 min for EPR measurement.

2.2. Calorimetry

We measured the actual power delivered to the solution with calorimetry, which is a standard method in dosimetry used both to measure power rates in various radiation fields and to calibrate standard and routine dosimeters [23,51]. The quantification of the temperature rise in calorimetric dosimeters provides a direct measurement of the absorbed power. A thermocouple (K type) measured the rise in temperature and we calculated the ultrasonic power dissipated in the solution by (Eq. 1):

$$Power\ (w) = \left(\frac{dT}{dt}\right) C_P m \quad (1)$$

Where C_p, m and (dT/dt) are respectively the specific heat capacity of the liquid ($J \cdot g^{-1} \cdot K^{-1}$)), the mass of the liquid (g) and the temperature difference per second ($K \cdot s^{-1}$).

This expression derives from the global calorimetric power dissipation after neglecting some parameters (Eq. 2): Calorimetric power dissipation = (Energy utilised to raise the temperature of bulk liquid) + (Energy absorbed by reactor walls and transducers) + (Energy lost to ambient air by convection) [52]:

$$P_{cal} = (mC_P\Delta T)_{liquid} + (m_i C_{pi}\Delta T)_{inner\ reactor\ wall} + (hA\Delta T) \quad (2)$$

Where m is the mass of liquid (g), m_i is the mass of the reactor/transducers (g), $C_p$is specific heat of liquid at constant pressure ($J.g^{-1}.K^{-1}$), C_{pi} is the specific heat of the material of the reactor ($J.g^{-1}.K^{-1}$), ΔT is the change in temperature (K), h is the convective heat transfer coefficient ($W.m^{-2}.K^{-1}$) and A is the area of the heat transfer (m^2).

We did not consider heat dissipated by the reactor walls and transducers, or the loss of energy in the ambient air due to convective heat transfer. Working at the laboratory scale with a volume of a few mL and small contact surface (liquid-wall, liquid-air), we can assume that heat losses by convection and conduction represent a negligible fraction of the global energy. These approximations result in about 5 % error on the measurement[17,52].

2.3. Electron Paramagnetic Resonance measurements and TEMPO calibration

We analyzed all the samples immediately after the sonication experiment, to avoid spin adduct decomposition. We transferred the 40 µL samples to 4 mm quartz EPR tubes to avoid paramagnetic impurities. A Bruker Elexsys E580 X-band EPR Spectrometer with 100 kHz modulation frequency and a microwave power level of 6.5 mW were used to record spectra. All spectra were recorded at room temperature. Each EPR measurement was repeated three times. Further parameters are given in Table 1. We used the SpinFit module in the Bruker Xepr software to simulate the spectra observed and thereby measure the hyperfine coupling constants to nitrogen (a_N) and hydrogen (a_H), which give information about the nature of trapped radicals.

We created a calibration curve from solutions of the stable radical 2,2,6,6-tetramethyl-1-piperidinyloxy (TEMPO) in trimethylene glycol to quantify spin adduct concentration. We prepared a 6-point calibration curve of TEMPO (Figure 1). We expressed the spin adduct yields

in concentration units by double integration of the simulated spectra and compared them with the double integrals of TEMPO peak areas at known concentrations (1 μM, 10 μM, 50 μM, 100 μM, 250 μM).

Table 1:Electron paramagnetic resonance experimental parameters.

Parameter	**Unit**	**Value**
Microwave frequency	GHz	9.7
Modulation frequency	kHz	100
Attenuation	dB	15
Microwave power	mW	6.5
Modulation amplitude	G	3
Time constant	s	1.28
Sweep time	s	83.89
Number of scans	-	3
Center field	G	3510.00

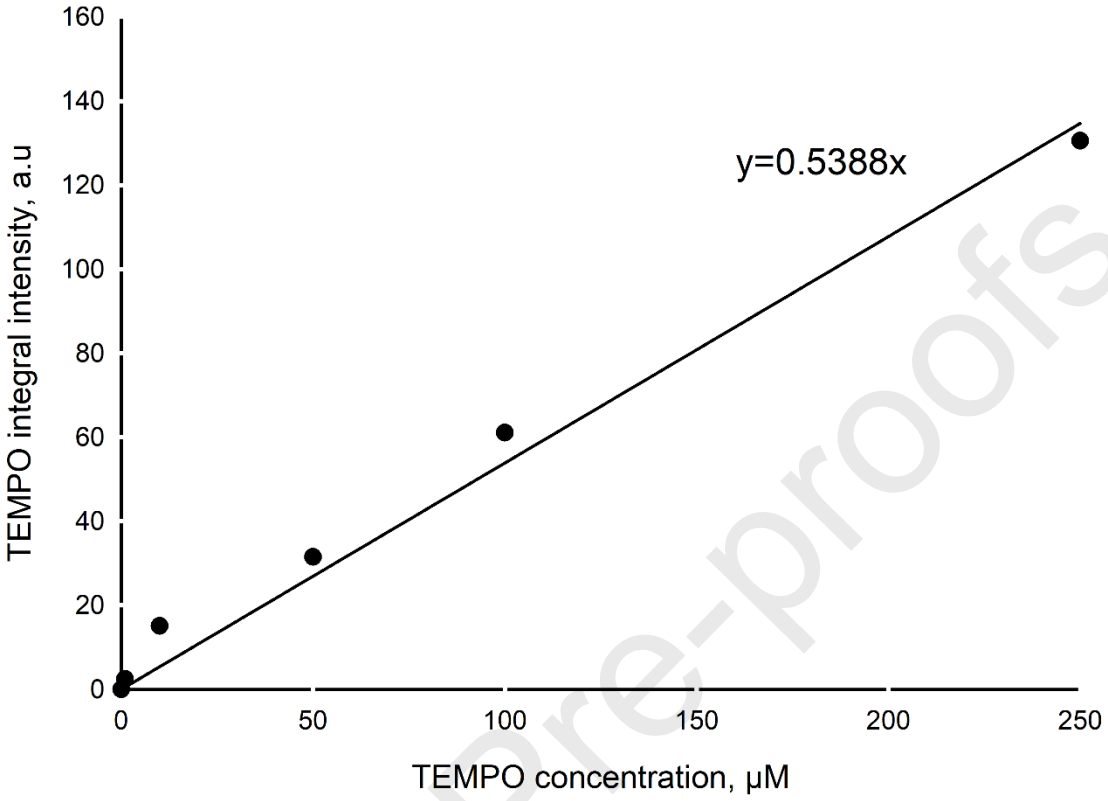

Figure 2: Standard curve relating double integrated intensity of TEMPO signal to concentration of TEMPO.

3. Results and discussion

3.1. EPR spectra and identification of radical adducts

The fragmentation of trimethylene glycol occurs mainly by breaking the C-C or C-O bonds. The possible radicals are: •CH_2OH, •CH_2CH_2OH, •$CH_2CH_2CH_2OH$ and •OH. The EPR spectrum (Figure 3) of the DMPO adduct generated in trimethylene glycol contains six lines as a result of hyperfine coupling to nitrogen (I=1, a_N=1.522 mT) and hydrogen (I=1/2, a_H^β = 2.171 mT) in the β position with respect to the nitrogen. The coupling to hydrogen is greater than that to nitrogen, indicating that the trapped radical is centred on a carbon atom [37,45]. Therefore, we excluded the detection of the hydroxyl radical •OH (a_N=1.42 mT and a_H^β = 1.16 mT in 1-octanol [53,54]). Moreover, the main information on the nature of the radicals trapped by DMPO comes from the value of the β hydrogen hyperfine coupling constant (a_H^β). Specifically, for alkyl radical adducts,

$a_H^\beta \geq 2.0$ mT, while $0.6 \geq a_H^\beta \geq 0.8$ mT for alkoxy radicals [40],[54],[55][56], [57]. This confirms the absence of an alkoxy radical. The values of the hyperfine coupling constants match those reported for the DMPO /Hydroxyalkyl radical adduct (Table 2) [41][58]. Therefore, we conclude that the spectra observed correspond to a Hydroxyalkyl radical.

Table 2: EPR Spectral Parameters for DMPO/ Hydroxyalkyl Radicals adduct

Radical	**Solvent**	a_N **,mT**	a_H^β**, mT**	**g**	**References**
•ROH	Trimethylene glycol	1.52	2.17	2.006	This work
•CH_2OH	Ethylene glycol	1.56	2.10	-	[45]
•CH_2OH	Water/methanol	1.59	2.26	2.0055	[41][58]
•CH_2OH	Water	1.58	2.23	2.0056-2.0062	[59]
•CH_2OH	Methanol	1.52	2.14	2.00563	[60]
•CH_2CH_2OH	water	1.598	2.28	2.0057	[54][56]
•$CH_2CH_2CH_2OH$	water	1.56	2.56	-	[61]

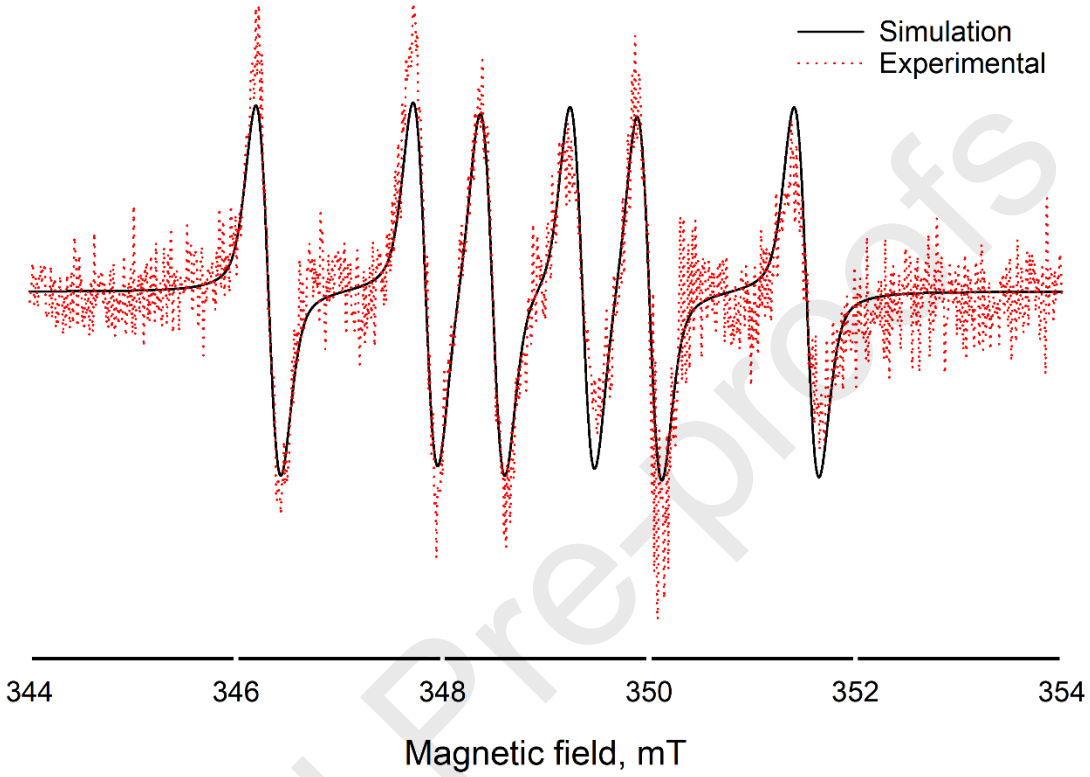

Figure 3: Comparison of simulated and experimental data (60 min of sonication in trimethylene glycol). Simulation parameters: a_N = 1.521 mT, a_H^β = 2.171 mT, g= 2.006.

3.2. Effect of SiO_2 particle size and concentration

When sonication starts, radicals form in our experimental conditions. We can detect radical adducts after 5 min of sonication and their concentration in the media increases with time (Figure 4). The concentrations reach a plateau between 30 min and 40 min of sonication (Figure 5 and 6), indicating that formation and decomposition of adducts are in equilibrium [62]. In a separate experiment, we tracked the decomposition rate of the radicals after sonication (lasted 60 min) stopped. After 105 min, there are no more radicals in the solution in the absence of solids (Figure 7).

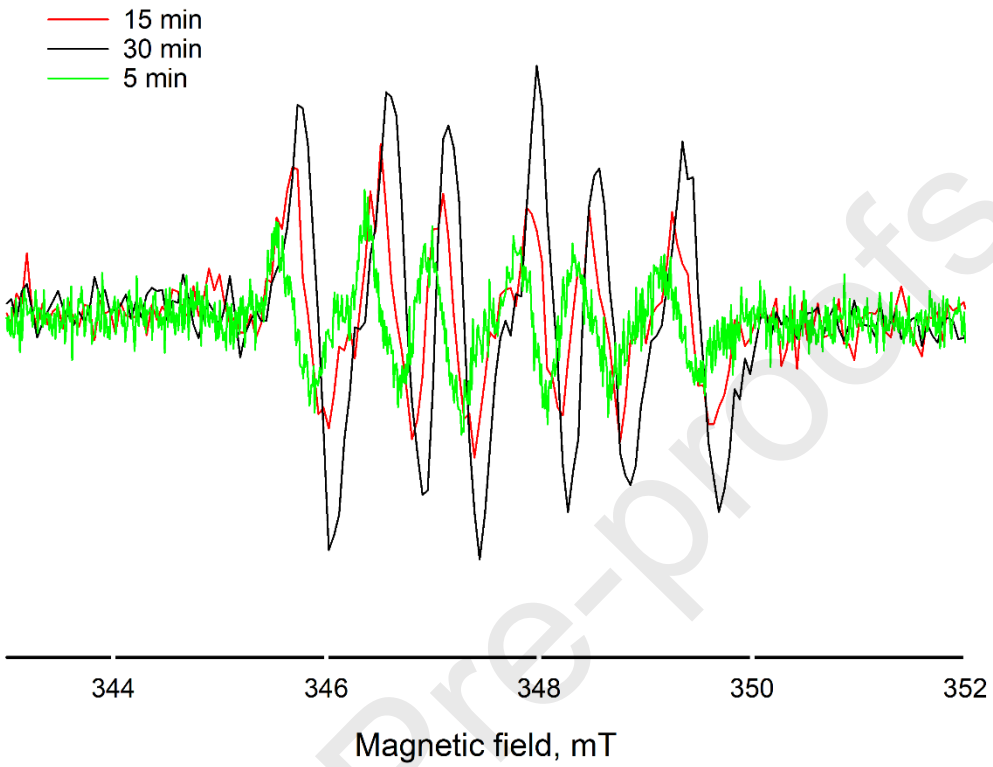

Figure 4: EPR spectra of radical adduct generated in trimethylene glycol. Spectra were acquired immediately after sonication for the period of time indicated in the figure legend. (US power= 24.7 W, T= 61 °C, particle diameter= 12-26 µm, 3 wt%)

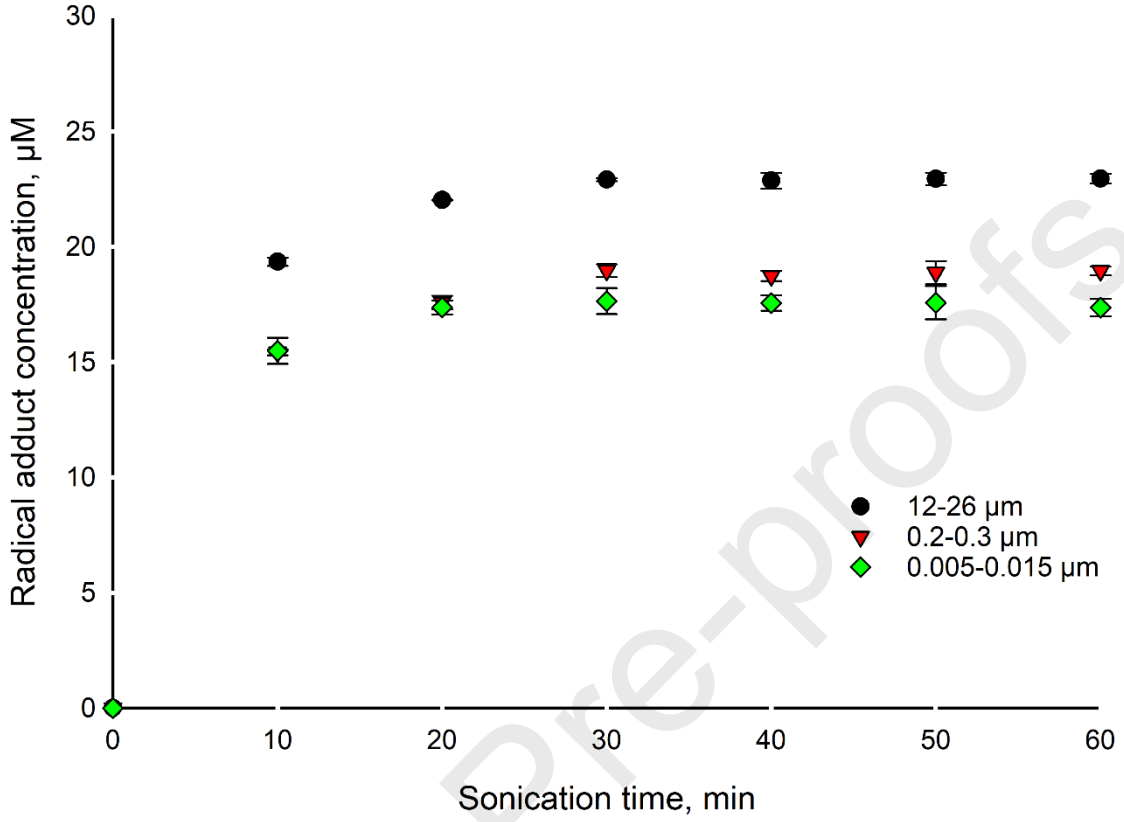

Figure 5: SiO_2 size effect with 3 wt% of solid and different particle size (in trimethylene glycol, US power= 24.7 W, T= 61 °C), error bars represent the sample standard deviation.

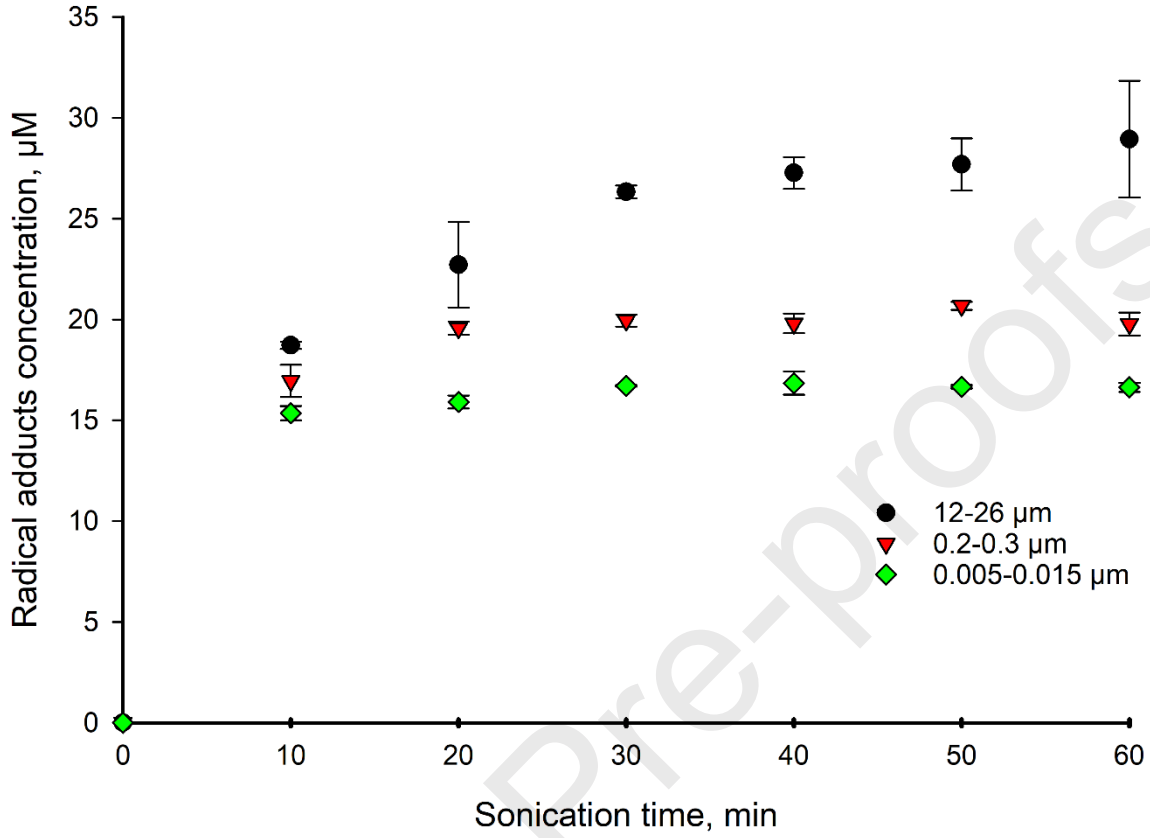

Figure 6: SiO_2 size effect with 0.5 %wt of solid and different particle size (in trimethylene glycol, US power= 24.7 W, T= 61 °C), error bars represent the sample standard deviation

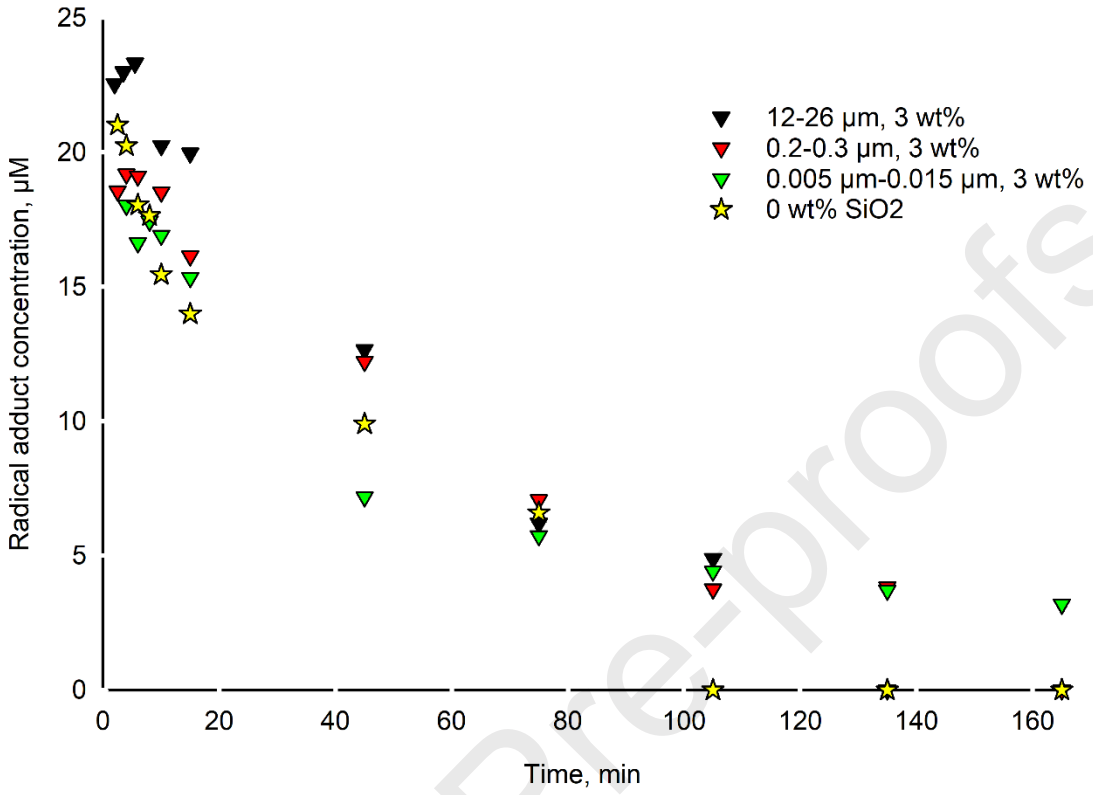

Figure 7: Radical adduct decomposition in the presence of SiO_2 particles of different size and at different concentrations following 60 min sonication in trimethylene glycol. In the plot, time t=0 indicates the end of the sonication period.

The size effect results (Figures 5 and 6) for both loadings of silica particles (3 wt% and 0.5 wt%) show that the concentration of radical adduct increases with particle size. For example, after 60 min sonication, the radical adduct concentration was twice as high for 12-26 µm than for 5-15 nm particles (for 0.5 wt% solids, 29 µM versus 16 µM, respectively). This can be rationalized in that the number of nucleation sites on the surface of the particles increases with an increase in their size, which produces more cavitation bubbles and subsequently more radicals. This is consistent with the results of Shanei, Tuziut and their coworkers [63] , [64]. They explained that the low chemical cavitation yield at the smallest size of particles is due to the fact that these particles and the fluid surrounding the bubbles were in motion together and that the particles do not necessarily

act as a rigid wall against the bubble implosion to cause an asymmetric collapse, leading to the generation of a large number of bubbles and subsequently a high number of radicals. In the case of particles in the nanometer range, the implosion of the acoustic bubbles creates micro-sized shear flows in different directions, whose diameter is larger than that of the solid particles. The solid particles are then surrounded by the jets of fluid, which scatter them in different directions. The greater the amount of solids in the solution, the higher the surface area available for nucleation and the higher the concentration of radicals formed. An increase in the surface area provides nucleation sites of bubbles active for cavitation. However, in our case, we obtained the opposite; for particle size of 12-26 μm and 0.2-0.3 μm, the concentration of 0.5 wt% produced more radical adducts than 3 wt% (Figure 8). Except for those with a diameter of 5-15 nm, there is no significant difference between the two concentrations. This is attributed to the high number of particles in the solution which can act as obstacles and slow down the propagation of ultrasound. A large concentration of solid particles dissipates the sound waves, which decreases the focused energy transferred into the system. Shanei [63] investigated the effect of the amount and size of gold nanoparticles on the acoustic cavitation activity to find a way for improving therapeutic effects on tumors. They found that the acoustic activity increases with the number of particles in the solution but beyond a certain amount (from 60 mg corresponding to 5 wt%), the activity begins decreasing. Barchouchi et al. [47] observed the same: the acoustic activity decreased sharply beyond a critical value between 0.01 and 0.03 m^2, depending on the size of the glass beads. Tuziuti et al. [64] considered the particle size effect on the absorbance of an aqueous KI solution with alumina particles (Al_2O_3) following sonolysis. When the added amount of particles increased beyond 20 mg, the absorbance became lower. They concluded that this is caused by the substantial prevention of ultrasound propagation due to the increase in the number of particles.

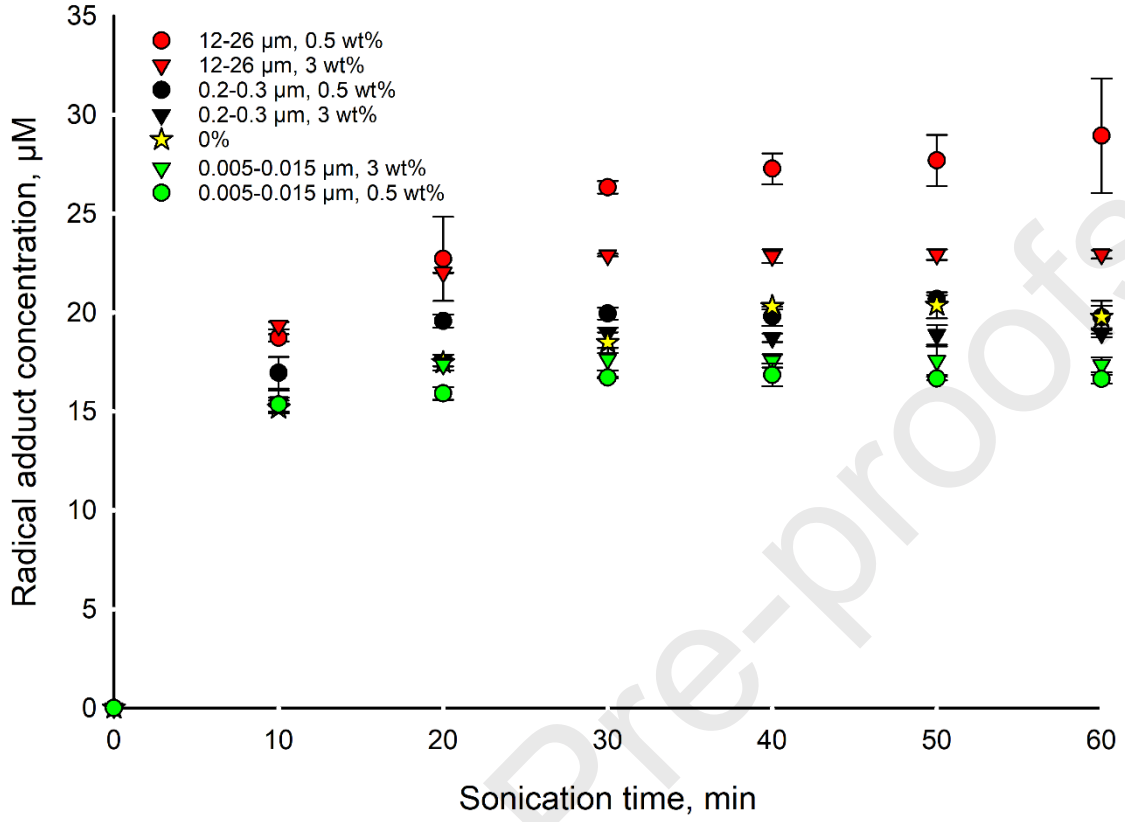

Figure 8: Effect of SiO_2 size and particle concentration (T= 61°C, US power= 24.7 W), error bars represent the sample standard deviation

3.3. Solvent effect

We find that the concentration of the radical adduct follows the same trend for both trimethylene glycol and propylene glycol (Figure 9). We are not therefore able to conclude which solvent has the best acoustic activity. However, theoretical studies indicated that liquids having a lower vapor pressure elicit a higher radical concentration[52], [65]. As the vapor pressure of the liquid increases, so does the vapor content of the cavity, thus lowering the energy released during the collapse. Thus the net cavitational effects will be lower for liquids with higher vapor pressure (vapor pressure of trimethylene glycol at 20 ºC = 0.006 kPa versus 0.011 kPa for propylene glycol) [52]. Also, liquids with higher surface tension, generally result in higher cavitational intensity

(surface tension at 20 °C of trimethylene glycol= 41.1 mN/m versus 38.0 mN/m for propylene glycol). Therefore, we chose trimethylene glycol to complete the rest of the experiments.

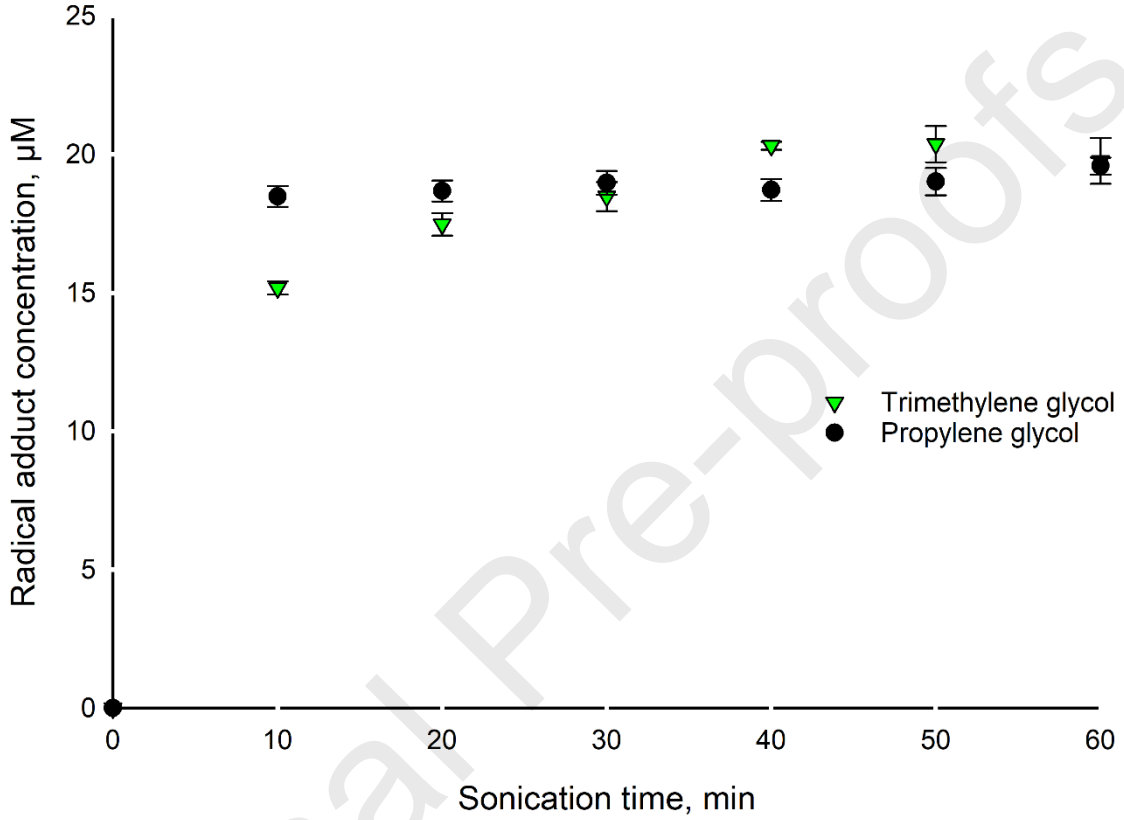

Figure 9: Comparison of the radical adduct concentration in trimethylene glycol and propylene glycol as a solvent (US power =24.7 W, 0% solid and T=61 °C), error bars represent the sample standard deviation.

3.4. Ultrasound power effect

The power delivered by the 500 W horn at 20 % and 40 % amplitude was 24.7 W and 50.6 W, respectively, according to the calorimetric calibration. As expected, the cavitation activity increases with the power of the sonication (Figure 10). With an increase in the intensity of irradiation, the collapse pressure increases, leading to enhanced cavitational effects. The size of

the cavity increases with the intensity of the irradiation; therefore, a more cavitationally active volume is achieved with a longer lifetime of the cavity [66],[67].

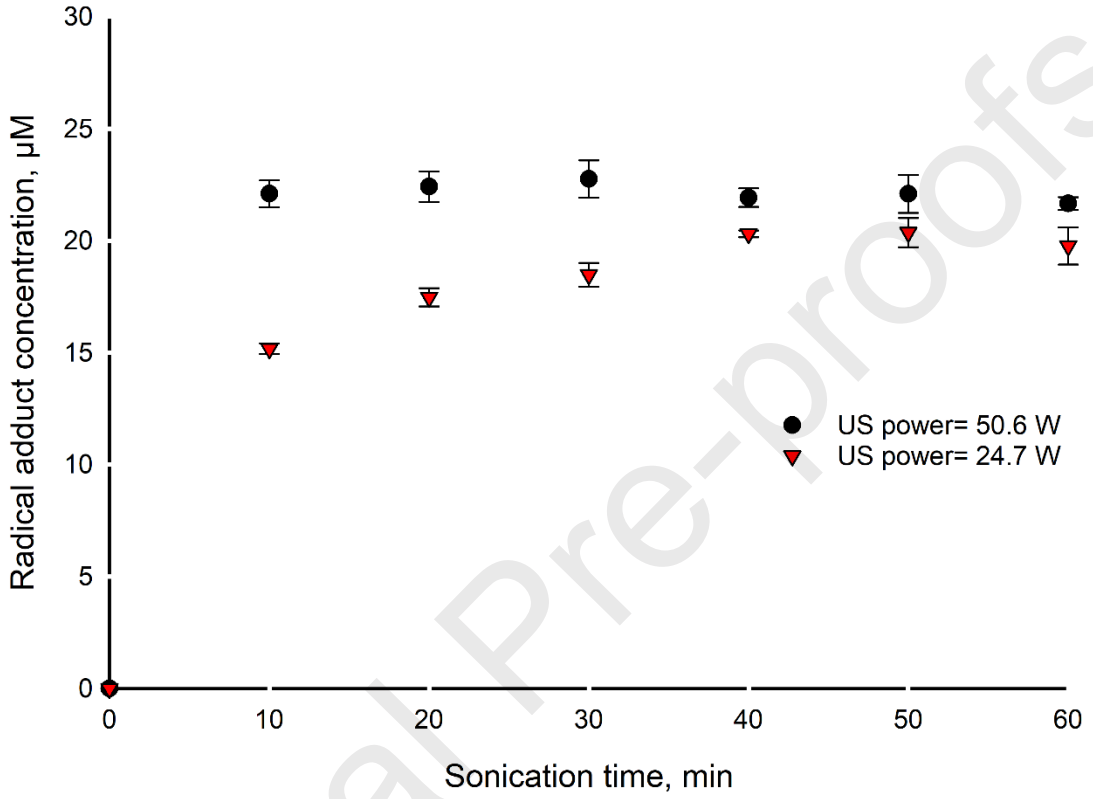

Figure 10: Ultrasound power effect (0% solid, T= 61 °C). Error bars represent the sample standard deviation.

3.5. Temperature effect

We expect the cavitational activity to decrease at higher operating temperature in the reactor. Price et al. [68] and many other [52], [66], [67], [69] interpret the cavitational activity in relation to the vapor pressure of the solvent, whereby there is a higher active gas nuclei concentration in the presence of solvents with a higher boiling point. This amortizes the collapse and reduces the shock waves. However, we obtained the opposite; we produced more radical adducts working at 75 °C than at 61 °C (27 µM vs 19 µM after 50 min of sonication) (Figure 11). This is attributed to the fact that higher operating temperature increases the vapor pressure inside the bubble, which in turn leads to a higher concentration of chemical species inside the cavitation bubble thereby generating

much higher amounts of free radicals in the system [66]. This increases reaction rates, which is of interest to our case, where chemical reactions will be occurring so we have to find an optimum operating temperature.

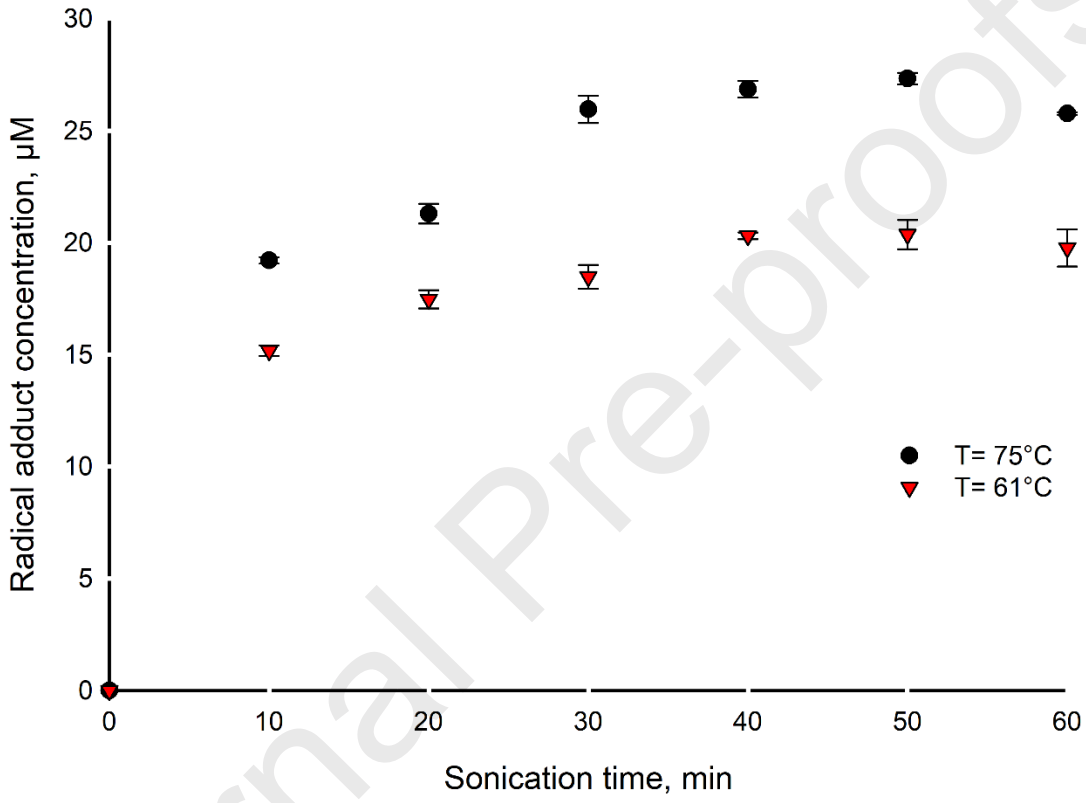

Figure 11: Temperature effect (US power= 24.7 W, 0% solid)

4. Conclusion

EPR is an effective tool for measuring the chemical effect threshold of the acoustic cavitation in organic solvents (trimethylene glycol and propylene glycol) and in the presence of SiO_2 particles with varying particle diameter and varying concentration. Pyrolysis in collapsing cavitation bubbles produced hydroxyalkyl radicals. Particles with 12-26 µm diameter produced the highest radical concentration (29 µM). The 0.5 wt% SiO_2 concentration gave higher cavitation activity than 3 wt% because a large number of particles can slow down the propagation of ultrasound.

These findings proved that adding particles of appropriate size and concentration has the potential to enhance the radical yield, and likely the overall acoustic pressure in selected reactor zones in sonochemical reactions. These findings have applications in the field of heterogeneous catalytic reactions, solid and particle processing, food and metal extractions, as well as for sonoprocessing in general.

Acknowledgments

This research was undertaken, in part, thanks to funding from the Canada Research Chair program. We are grateful to Prof. Martin G. Bakker from the Department of Chemistry and Biochemistry of the University of Alabama, for his valuable help and suggestions to improve the experimental conditions of this work and to Jean-Marc Gauthier of McGill University for providing lab space.

References

[1] S. V. Sancheti and P. R. Gogate, "A review of engineering aspects of intensification of chemical synthesis using ultrasound," *Ultrasonics Sonochemistry*, vol. 36. Elsevier B.V., pp. 527–543, May 01, 2017, doi: 10.1016/j.ultsonch.2016.08.009.

[2] D. C. Boffito, E. Martinez-Guerra, V. G. Gude, and G. S. Patience, "Conversion of refined and waste oils by ultrasound-assisted heterogeneous catalysis #30," in *Handbook of Ultrasonics and Sonochemistry*, Springer Singapore, 2016, pp. 931–963.

[3] T. S. Awad, H. A. Moharram, O. E. Shaltout, D. Asker, and M. M. Youssef, "Applications of ultrasound in analysis, processing and quality control of food: A review," *Food Research International*, vol. 48, no. 2. Elsevier, pp. 410–427, Oct. 01, 2012, doi: 10.1016/j.foodres.2012.05.004.

[4] N. Bhargava, R. S. Mor, K. Kumar, and V. S. Sharanagat, "Advances in application of ultrasound in food processing: A review," *Ultrasonics Sonochemistry*, vol. 70. Elsevier B.V., p. 105293, Jan. 01, 2021, doi: 10.1016/j.ultsonch.2020.105293.

[5] S. Mitragotri and J. Kost, "Low-frequency sonophoresis: A review," *Adv. Drug Deliv. Rev.*, vol. 56, no. 5, pp. 589–601, Mar. 2004, doi: 10.1016/j.addr.2003.10.024.

[6] A. Ahmadi *et al.*, "Recent advances in ultrasound-triggered drug delivery through lipid-based nanomaterials," *Drug Discovery Today*, vol. 25, no. 12. Elsevier Ltd, pp. 2182–2200, Dec. 01, 2020, doi: 10.1016/j.drudis.2020.09.026.

[7] D. Schieppati, F. Galli, M. L. Peyot, V. Yargeau, C. L. Bianchi, and D. C. Boffito, "An ultrasound-assisted photocatalytic treatment to remove an herbicidal pollutant from wastewaters," *Ultrason. Sonochem.*, vol. 54, pp. 302–310, Jun. 2019, doi: 10.1016/j.ultsonch.2019.01.027.

[8] X. Lu *et al.*, "A Review on Additives-assisted Ultrasound for Organic Pollutants Degradation," *Journal of Hazardous Materials*, vol. 403. Elsevier B.V., p. 123915, Feb. 05, 2021, doi: 10.1016/j.jhazmat.2020.123915.

[9] Z. Khani, D. Schieppati, C. L. Bianchi, and D. C. Boffito, "The Sonophotocatalytic Degradation of Pharmaceuticals in Water by MnOx-TiO2 Systems with Tuned Band-Gaps," *Catalysts*, vol. 9, no. 11, p. 949, Nov. 2019, doi: 10.3390/catal9110949.

[10] E. V. Rokhina, P. Lens, and J. Virkutyte, "Low-frequency ultrasound in biotechnology: state of the art," *Trends in Biotechnology*, vol. 27, no. 5. Elsevier Current Trends, pp. 298–306, May 01, 2009, doi: 10.1016/j.tibtech.2009.02.001.

[11] B. A. Bhanvase and S. H. Sonawane, "Ultrasound assisted in situ emulsion polymerization for polymer nanocomposite: A review," *Chemical Engineering and Processing: Process Intensification*, vol. 85. Elsevier, pp. 86–107, Nov. 01, 2014, doi: 10.1016/j.cep.2014.08.007.

[12] D. C. Boffito and D. Fernandez Rivas, “Process intensification connects scales and disciplines towards sustainability,” *Can. J. Chem. Eng.*, p. cjce.23871, Oct. 2020, doi: 10.1002/cjce.23871.

[13] M. Ashokkumar *et al.*, *Handbook of ultrasonics and sonochemistry*. Springer Singapore, 2016.

[14] K. S. Suslick and S. E. Skrabalak, “Sonocatalysis,” in *Handbook of Heterogeneous Catalysis*, Weinheim, Germany: Wiley-VCH Verlag GmbH & Co. KGaA, 2008, pp. 2007–2017.

[15] T. J. Mason and A. Tiehm, *Advances in Sonochemistry, Volume 6.* Elsevier, 2001.

[16] KS Suslick, “The chemical effects of ultrasound,” *Sci. Am.*, vol. 260, no. 2, pp. 80–87, 1989, Accessed: Apr. 16, 2020. [Online]. Available: https://www.jstor.org/stable/24987145.

[17] S. Koda, T. Kimura, T. Kondo, and H. Mitome, “A standard method to calibrate sonochemical efficiency of an individual reaction system,” *Ultrason. Sonochem.*, vol. 10, no. 3, pp. 149–156, May 2003, doi: 10.1016/S1350-4177(03)00084-1.

[18] A. H. Barati, M. Mokhtari -Dizaji, H. Mozdarani, S. Z. Bathaei, and Z. M. Hassan, “Free hydroxyl radical dosimetry by using 1 MHz low level ultrasound waves,” International Journal of Radiation Research, 2006.

[19] G. Chatel and J. C. Colmenares, “Sonochemistry: from Basic Principles to Innovative Applications,” *Topics in Current Chemistry*, vol. 375, no. 1. Springer Verlag, pp. 1–4, Feb. 01, 2017, doi: 10.1007/s41061-016-0096-1.

[20] D. C. Boffito, F. Galli, C. Pirola, C. L. Bianchi, and G. S. Patience, "Ultrasonic free fatty acids esterification in tobacco and canola oil," in *Ultrasonics Sonochemistry*, Nov. 2014, vol. 21, no. 6, pp. 1969–1975, doi: 10.1016/j.ultsonch.2014.01.026.

[21] D. C. Boffito, S. Mansi, J. M. Leveque, C. Pirola, C. L. Bianchi, and G. S. Patience, "Ultrafast biodiesel production using ultrasound in batch and continuous reactors," *ACS Sustain. Chem. Eng.*, vol. 1, no. 11, pp. 1432–1439, Nov. 2013, doi: 10.1021/sc400161s.

[22] T. J. Mason, J. P. Lorimer, D. M. Bates, and Y. Zhao, "Dosimetry in sonochemistry: the use of aqueous terephthalate ion as a fluorescence monitor," *Ultrason. - Sonochemistry*, vol. 1, no. 2, pp. S91–S95, Jan. 1994, doi: 10.1016/1350-4177(94)90004-3.

[23] W. L. McLaughlin, A. Miller, A. Kovács, and K. K. Mehta, "Dosimetry Methods," in *Handbook of Nuclear Chemistry*, Springer US, 2011, pp. 2287–2318.

[24] M. O'Leary *et al.*, "Observation of dose-rate dependence in a Fricke dosimeter irradiated at low dose rates with monoenergetic X-rays," *Sci. Rep.*, vol. 8, no. 1, pp. 1–9, Dec. 2018, doi: 10.1038/s41598-018-21813-z.

[25] A. K. Jana and S. N. Chatterjee, "Estimation of hydroxyl free radicals produced by ultrasound in Fricke solution used as a chemical dosimeter," *Ultrason. - Sonochemistry*, vol. 2, no. 2, pp. S87–S91, Jan. 1995, doi: 10.1016/1350-4177(95)00025-2.

[26] Y. Iida, K. Yasui, T. Tuziuti, and M. Sivakumar, "Sonochemistry and its dosimetry," in *Microchemical Journal*, Jun. 2005, vol. 80, no. 2, pp. 159–164, doi: 10.1016/j.microc.2004.07.016.

[27] A. Ebrahiminia, M. Mokhtari-Dizaji, and T. Toliyat, "Dual frequency cavitation event

sensor with iodide dosimeter," *Ultrason. Sonochem.*, vol. 28, pp. 276–282, Aug. 2016, doi: 10.1016/j.ultsonch.2015.07.005.

[28] D. B. Rajamma, S. Anandan, N. S. M. Yusof, B. G. Pollet, and M. Ashokkumar, "Sonochemical dosimetry: A comparative study of Weissler, Fricke and terephthalic acid methods," *Ultrason. Sonochem.*, vol. 72, p. 105413, Apr. 2021, doi: 10.1016/j.ultsonch.2020.105413.

[29] A. Weissler, "Formation of Hydrogen Peroxide by Ultrasonic Waves: Free Radicals," *J. Am. Chem. Soc.*, vol. 81, no. 5, pp. 1077–1081, 1959, doi: 10.1021/ja01514a015.

[30] G. Mark *et al.*, "OH-radical formation by ultrasound in aqueous solution - Part II: Terephthalate and Fricke dosimetry and the influence of various conditions on the sonolytic yield," *Ultrason. Sonochem.*, vol. 5, no. 2, pp. 41–52, Jun. 1998, doi: 10.1016/S1350-4177(98)00012-1.

[31] A. Ebrahiminia, M. Mokhtari-Dizaji, and T. Toliyat, "Correlation between iodide dosimetry and terephthalic acid dosimetry to evaluate the reactive radical production due to the acoustic cavitation activity," *Ultrason. Sonochem.*, vol. 20, no. 1, pp. 366–372, Jan. 2013, doi: 10.1016/j.ultsonch.2012.05.016.

[32] M. P. Brenner, S. Hilgenfeldt, and D. Lohse, "Single-bubble sonoluminescence," *Reviews of Modern Physics*, vol. 74, no. 2. American Physical Society, pp. 425–484, May 13, 2002, doi: 10.1103/RevModPhys.74.425.

[33] H. Hasanzadeh, M. Mokhtari-Dizaji, S. Zahra Bathaie, Z. M. Hassan, V. Nilchiani, and H. Goudarzi, "Enhancement and control of acoustic cavitation yield by low-level dual frequency sonication: A subharmonic analysis," *Ultrason. Sonochem.*, vol. 18, no. 1, pp.

394–400, 2011, doi: 10.1016/j.ultsonch.2010.07.005.

[34] W. Lauterborn and W. Hentschel, “Cavitation bubble dynamics studied by high speed photography and holography: part one,” *Ultrasonics*, vol. 23, no. 6, pp. 260–268, Nov. 1985, doi: 10.1016/0041-624X(85)90048-4.

[35] V. Mišík and P. Riesz, “EPR study of free radicals induced by ultrasound in organic liquids II. Probing the temperatures of cavitation regions,” *Ultrason. Sonochem.*, vol. 3, no. 1, pp. 25–37, Feb. 1996, doi: 10.1016/1350-4177(95)00036-4.

[36] Q. A. Zhang, Y. Shen, X. H. Fan, J. F. G. Martín, X. Wang, and Y. Song, “Free radical generation induced by ultrasound in red wine and model wine: An EPR spin-trapping study,” *Ultrason. Sonochem.*, vol. 27, pp. 96–101, Nov. 2015, doi: 10.1016/j.ultsonch.2015.05.003.

[37] R. Lauricella and B. Tuccio, “Detection and characterisation of free radicals after spin trapping,” in *Electron Paramagnetic Resonance Spectroscopy: Applications*, Springer International Publishing, 2020, pp. 51–82.

[38] V. Migik and P. Riesz, “Recent applications of EPR and spin trapping to sonochemical studies of organic liquids and aqueous solutions,” ELSEVIER, 1996.

[39] G. R. Eaton, S. S. Eaton, D. P. Barr, and R. T. Weber, *Quantitative EPR*. Springer, 2010.

[40] R. L. Blakley, D. D. Henry, W. T. Morgan, W. L. Clapp, C. J. Smith, and D. Barr, “Quantitative electron paramagnetic resonance: The importance of matching the Q-factor of standards and samples,” *Appl. Spectrosc.*, vol. 55, no. 10, pp. 1375–1381, 2001, doi: 10.1366/0003702011953504.

[41] M. Brustolon and E. Giamello, *Electron Paramagnetic Resonance: A Practitioner's Toolkit*. 2008.

[42] P. Bertrand and P. Bertrand, "The Electron Paramagnetic Resonance Phenomenon," in *Electron Paramagnetic Resonance Spectroscopy*, Springer International Publishing, 2020, pp. 3–30.

[43] L. Xu *et al.*, "Mechanistic study on the combination of ultrasound and peroxymonosulfate for the decomposition of endocrine disrupting compounds," *Ultrason. Sonochem.*, vol. 60, p. 104749, Jan. 2020, doi: 10.1016/j.ultsonch.2019.104749.

[44] Z. Wei, F. A. Villamena, and L. K. Weavers, "Kinetics and Mechanism of Ultrasonic Activation of Persulfate: An in Situ EPR Spin Trapping Study," *Environ. Sci. Technol.*, vol. 51, no. 6, pp. 3410–3417, Mar. 2017, doi: 10.1021/acs.est.6b05392.

[45] M. M. Castellanos, D. Reyman, C. Sieiro, and P. Calle, "ESR-spin trapping study on the sonochemistry of liquids in the presence of oxygen. Evidence for the superoxide radical anion formation.," *Ultrason. Sonochem.*, vol. 8, no. 1, pp. 17–22, Jan. 2001, doi: 10.1016/s1350-4177(99)00047-4.

[46] D. C. Boffito and T. Van Gerven, "Process Intensification and Catalysis," in *Reference Module in Chemistry, Molecular Sciences and Chemical Engineering*, Elsevier, 2019.

[47] A. Barchouchi, S. Molina-Boisseau, N. Gondrexon, and S. Baup, "Sonochemical activity in ultrasonic reactors under heterogeneous conditions," *Ultrason. Sonochem.*, vol. 72, p. 105407, Apr. 2021, doi: 10.1016/j.ultsonch.2020.105407.

[48] K. M. Schaich, "EPR Methods for Studying Free Radicals in Foods," *ACS Symp. Ser.*, vol.

807, pp. 12–34, 2002, doi: 10.1021/bk-2002-0807.ch002.

[49] K. Abbas, N. Babić, and F. Peyrot, “Use of spin traps to detect superoxide production in living cells by electron paramagnetic resonance (EPR) spectroscopy,” *Methods*, vol. 109. Academic Press Inc., pp. 31–43, Oct. 15, 2016, doi: 10.1016/j.ymeth.2016.05.001.

[50] F. J. Barba *et al.*, “Electron spin resonance as a tool to monitor the influence of novel processing technologies on food properties,” *Trends Food Sci. Technol.*, vol. 100, pp. 77–87, Mar. 2020, doi: 10.1016/j.tifs.2020.03.032.

[51] T. Kikuchi and T. Uchida, “Calorimetric method for measuring high ultrasonic power using water as a heating material,” *J. Phys. Conf. Ser.*, vol. 279, p. 012012, Feb. 2011, doi: 10.1088/1742-6596/279/1/012012.

[52] P. R. Gogate, V. S. Sutkar, and A. B. Pandit, “Sonochemical reactors: Important design and scale up considerations with a special emphasis on heterogeneous systems,” *Chem. Eng. J.*, vol. 166, no. 3, pp. 1066–1082, Feb. 2011, doi: 10.1016/j.cej.2010.11.069.

[53] Y. K. Zhang, D. H. Lu, and G. Z. Xu, “Synthesis and Plane Selective Spin Trapping of a Novel Trap 5, 5-Dimethy l-3-(2-ethoxycarbony lethyl)-1 -pyrroline N-oxide,” *Zeitschrift fur Naturforsch. - Sect. B J. Chem. Sci.*, vol. 45, no. 7, pp. 1075–1083, Jul. 1990, doi: 10.1515/znb-1990-0729.

[54] G. R. Buettner, “Spin Trapping: ESR parameters of spin adducts,” *Free Radical Biology and Medicine*, vol. 3, no. 4. Pergamon, pp. 259–303, Jan. 01, 1987, doi: 10.1016/S0891-5849(87)80033-3.

[55] P. Bilski, C. F. Chignell, J. Szychlinski, A. Borkowski, E. Oleksy, and K. Reszka,

"Photooxidation of Organic and Inorganic Substrates during UV Photolysis of Nitrite Anion in Aqueous Solution," *J. Am. Chem. Soc.*, vol. 114, no. 2, pp. 549–556, Jan. 1992, doi: 10.1021/ja00028a023.

[56] Y. KIRINO, T. OHKUMA, and T. KWAN, "Spin trapping with 5,5-dimethylpyrroline-N-oxide in aqueous solution.," *Chem. Pharm. Bull. (Tokyo).*, vol. 29, no. 1, pp. 29–34, Jan. 1981, doi: 10.1248/cpb.29.29.

[57] H. Taniguchi and K. P. Madden, "DMPO-alkyl radical spin trapping: An in situ radiolysis steady-state ESR study," *Radiat. Res.*, vol. 153, no. 4, pp. 447–453, 2000, doi: 10.1667/0033-7587(2000)153[0447:DARSTA]2.0.CO;2.

[58] G. R. Buettner, "Spin Trapping: ESR parameters of spin adducts 1474 1528V," *Free Radical Biology and Medicine*, vol. 3, no. 4. Pergamon, pp. 259–303, Jan. 01, 1987, doi: 10.1016/S0891-5849(87)80033-3.

[59] R. Konaka, M. Kawai, H. Noda, M. Kohno, and R. Niwa, "Synthesis and evaluation of DMPO-type spin traps," *Free Radic. Res.*, vol. 23, no. 1, pp. 15–25, 1995, doi: 10.3109/10715769509064015.

[60] D. L. Haire, Y. Kotake, and E. G. Janzen, "An EPR/ENDOR study of aminoxyls (nitroxides) capable of intramolecular bonding: hydroxyalkyl radical spin adducts of nitrones," *Can. J. Chem.*, vol. 66, no. 8, pp. 1901–1911, Aug. 1988, doi: 10.1139/v88-307.

[61] R. Sato *et al.*, "Syntheses and spin trappings of 3-hydroxymethyl-5,5-dimethyl-1-pyrroline N-oxide and 3-(3-hydroxypropyl)-5,5-dimethyl-1-pyrroline N-oxide," *Chem. Lett.*, no. 10, pp. 1059–1060, Nov. 1997, doi: 10.1246/cl.1997.1059.

[62] M. Kubo, K. Sekiguchi, N. Shibasaki-Kitakawa, and T. Yonemoto, "Kinetic model for formation of DMPO-OH in water under ultrasonic irradiation using EPR spin trapping method," *Res. Chem. Intermed.*, 2012, doi: 10.1007/s11164-012-0536-7.

[63] A. Shanei and M. M. Shanei, "Effect of gold nanoparticle size on acoustic cavitation using chemical dosimetry method," *Ultrason. Sonochem.*, vol. 34, pp. 45–50, Jan. 2017, doi: 10.1016/j.ultsonch.2016.05.010.

[64] T. Tuziuti, K. Yasui, M. Sivakumar, Y. Iida, and N. Miyoshi, "Correlation between acoustic cavitation noise and yield enhancement of sonochemical reaction by particle addition," *J. Phys. Chem. A*, vol. 109, no. 21, pp. 4869–4872, Jun. 2005, doi: 10.1021/jp0503516.

[65] P. R. Gogate and A. B. Pandit, "Sonochemical reactors: Scale up aspects," in *Ultrasonics Sonochemistry*, May 2004, vol. 11, no. 3–4, pp. 105–117, doi: 10.1016/j.ultsonch.2004.01.005.

[66] V. S. Sutkar and P. R. Gogate, "Design aspects of sonochemical reactors: Techniques for understanding cavitational activity distribution and effect of operating parameters," *Chemical Engineering Journal*, vol. 155, no. 1–2. Elsevier, pp. 26–36, Dec. 01, 2009, doi: 10.1016/j.cej.2009.07.021.

[67] A. V. Prabhu, P. R. Gogate, and A. B. Pandit, "Optimization of multiple-frequency sonochemical reactors," in *Chemical Engineering Science*, Nov. 2004, vol. 59, no. 22–23, pp. 4991–4998, doi: 10.1016/j.ces.2004.09.033.

[68] G. J. Price and P. F. Smith, "Ultrasonic degradation of polymer solutions: 2. The effect of temperature, ultrasound intensity and dissolved gases on polystyrene in toluene," *Polymer*

(Guildf)., vol. 34, no. 19, pp. 4111–4117, Jan. 1993, doi: 10.1016/0032-3861(93)90675-Z.

[69] D. C. Boffito *et al.*, "Ultrasonic enhancement of the acidity, surface area and free fatty acids esterification catalytic activity of sulphated ZrO2-TiO2 systems," *J. Catal.*, vol. 297, pp. 17–26, Jan. 2013, doi: 10.1016/j.jcat.2012.09.013.

Author statement

Hela Laajimi: Methodology, Validation, Formal analysis, Investigation, Data Curation, Writing - Original Draft, Writing - Review & Editing, Visualization

Michela Mattia: Methodology, Validation, Formal analysis, Investigation, Data Curation, Writing - Original Draft

Robin Stein: Methodology, Formal analysis, Resources, Investigation, Data Curation, Writing - Original Draft, Supervision

Claudia L. Bianchi: Formal analysis, Resources, Writing - Original Draft, Supervision

Daria C. Boffito: Conceptualization, Methodology, Formal analysis, Resources, Writing - Original Draft, Supervision, Writing - Review & Editing, Project administration, Funding acquisition